Applied Research

Applied Research

RESEARCH ARTICLE OPEN ACCESS

Dot-by-Dot Printing of Capacitors by Lift

Stefan Lux[1] | Nadezda Kuznetsova[2] | Ajeya R. Simha[1] | Dario Mager[1] | Frank Breitling[1] | Jan G. Korvink[1]

[1]Institute of Microstructure Technology (IMT)—Karlsruhe Institute of Technology (KIT), Eggenstein-Leopoldshafen, Germany | [2]Department of Electrical Engineering (ESAT), Micro and Nano Systems (MNS), KU Leuven, Leuven, Belgium

Correspondence: Frank Breitling (frank.breitling@kit.edu)

Received: 30 September 2024 | **Revised:** 6 December 2024 | **Accepted:** 10 December 2024

Funding: The authors acknowledge the support from the EU under the NANOSTACKS project EXCELLENT SCIENCE— Future and Emerging Technologies (FET) (ID: 951949) for financial support. The authors acknowledge support from the Deutsche Forschungsgemeinschaft (DFG) under Germany's Excellence Strategy—3DMM2O (EXC-2082/1-390761711). We further acknowledge support from the Helmholtz Society's program Materials Systems Engineering, in the Research Area Information.

Keywords: capacitor | laser-induced forward transfer | LIFT | rapid prototyping

ABSTRACT

Capacitors play a crucial role in modern electronics as they are widely employed for energy storage, signal processing, radiofrequency tuning and matching, and signal filtering. This paper presents a novel approach to chip-scale capacitor fabrication utilizing the laser-induced forward transfer (LIFT) technique, a versatile 3D printing method that offers a flexible and cost-effective alternative to conventional manufacturing processes. Plate capacitors were fabricated through dot-by-dot printing of titanium di-oxide and silver paste layers, and their performance evaluated. Optimal dot circularity at a diameter of 130 μm were achieved with printing parameters of 120 mW for 4 ms, with no noticeable surface defects. Using smaller dots enabled higher resolution, but this compromised the quality of the printed surface. The fabricated capacitors demonstrated a mean capacity of 40.1 ± 2.2 pF at 100 MHz, making them suitable also for high-frequency applications. The resistivity of the printed silver tracks was 1.2×10^{-7} Ωm, measured over 16 structures, and closely matched the manufacturer's specifications for the silver ink. The achieved resolution from the dot-by-dot method used in this paper provided greater flexibility in transfer in comparison to previously reported results using a square-shaped transfer geometry.

1 | Introduction

The manufacturing technology for capacitors has undergone significant advancements, leading to the successful implementation of a large number of approaches [1–3]. The silicon-based industry, in particular, has played a crucial role in providing a diverse range of high-performance electrical components [4, 5]. However, alongside established silicon-based manufacturing, printing technology has emerged as a promising alternative in the field of electronics [6]. This technology offers several advantages including rapid adaptability and a simplified manufacturing process that eliminates the need for cleanroom facilities. By leveraging printing technology, the production of capacitors can be made more efficient and cost-effective on a small scale, opening up new possibilities for the electronics industry.

In the field of printable electronics and additive manufacturing, various techniques are employed [7], each with its own set of advantages and disadvantages. One such technique is inkjet printing, which allows printing on flexible substrates and facilitates the fabrication of resistors, coils, sensors, and other components and devices. Inkjet printing offers a wide range of applications [8], limited primarily by printing time and ink properties [9]. To be suitable for inkjet printing, inks must possess stability and low viscosity to facilitate printhead usage [10] but have a high particle loading to enable the printing of structures with significant height. In addition, the surface

energy of the receiving substrate plays a crucial role because of the low viscosity of the ink.

Laser-induced forward transfer (LIFT) is a versatile method discovered in the late 1960s and the early 1970s [11]. Despite being developed for manufacturing purposes, it is often overshadowed by other manufacturing techniques. However, LIFT offers significant advantages, including the operational simplicity of its device and setup as well as the versatility in the types of inks it can accommodate, such as the ability to print materials in the form of solids, low- or high-viscosity inks, pastes, gels, and even polymers. Usually, these materials are prepared in the form of thin films on a donor substrate.

Researchers have successfully transferred minute droplets and multilayered pixels using LIFT technology. In 2009, Serra et al. pioneered the application of LIFT for transferring liquids [12]. They employed an additional layer to absorb laser irradiation, allowing for the successful transfer of a transparent solution consisting of water, glycerol, and a surfactant in the form of small droplets. Subsequent publications [13] investigated the transfer mechanism in detail. Following these studies, additional publications [14, 15] showed the transfer of silver paste by LIFT and provided a comprehensive analysis of the different transfer regimes, which depended on the laser fluence. The diverse applications and advancements in LIFT have been extensively reviewed and summarized by Serra and Piqué [16]. The versatility of this method is remarkable. Several publications have demonstrated the use of LIFT for fabricating electronic devices such as OLEDs and capacitors [17, 18]. In these methods, a pulsed UV laser source and sacrificial layer were employed to extract and propel a rectangular multilayered pixel onto the receiving substrate.

This work aims to demonstrate the printing of a pico-farad capacitor through additive manufacturing without the need to prefabricate multilayered pixels. This provides more freedom in the design and properties of the printed devices. To achieve this, a horizontal dielectric material and electrode were printed dot-by-dot on a conductive substrate. To evaluate the transfer process, a Dual Focused Ion Beam Scanning Electron Microscope (FIB-SEM) was used to generate cross-sectional views. Conductivity measurements were performed to evaluate the performance of the ink, and the capacitor function was investigated with a network analyzer (Agilent E5061B). The characterization tools provided evidence of the successful printing of capacitors. It is worth noting that the printing of a capacitor represents just one step toward the larger goal of printing various devices and sensors, and ultimately entire circuits. This approach offers significant design freedom and flexibility in terms of materials, enabling the exploration of diverse applications with few limitations.

2 | Materials and Methods

2.1 | LIFT System

LIFT was employed for the localized transfer of diverse paste materials. LIFT setups exist in various configurations with different laser sources. In our study, a diode laser with a wavelength of 405 nm (iBeam smart 405-S, TOPTICA Photonics AG, Munich, Germany) was used in combination with a two-mirrored laser scan head (intelliSCAN III 10, SCANLAB GmbH, Puchheim, Germany) to provide a localized transfer of paste material. As depicted in Figure 1b, the laser beam was directed by the laser scan head onto the stacked configuration of donor and acceptor slides and was focused by an F-Theta lens (JENar 170-355-140, JENOPTIK Optical Systems GmbH, Jena, Germany) onto the substrate. Figure 1a gives an impression of the real setup. Additionally to the described components a heating and cooling system was installed, that was used to keep the transfer conditions stable.

When the laser is focused on the donor material, the laser energy is absorbed by the transfer material, in this case, either

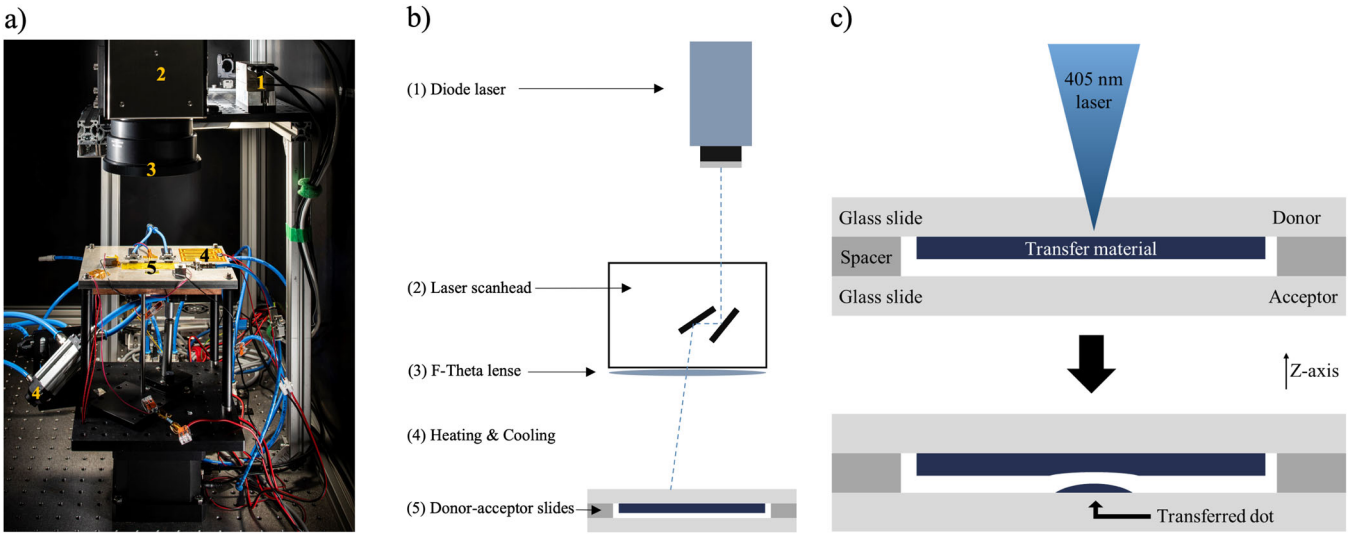

FIGURE 1 | (a) Image of the actual setup. (b) Schematic diagram of the LIFT setup: A 405-nm diode laser is directed by a laser scanhead and focused by an F-Theta lens onto the donor slide, resulting in a localized transfer of material. (c) The donor slide and acceptor slide are stacked over each other, separated by a defined spacer to keep them apart. The donor slide is covered with a thin layer of transfer material, such as a nanoparticle paste. The laser light heats a small region on the slide for a few milliseconds, leading to the transfer of a material dot onto the acceptor slide.

silver or titanium di-oxide paste. The transfer of these materials by LIFT is a well-established process described in the literature [15]. Previous studies have detailed how the interaction between laser fluence, the gap distance, and the thickness of the donor layer affects the transfer process.

For our purposes, the described "concrete-dot-transfer" type is the desired outcome because it produces round, uniform material dots. This type of transfer occurs when the donor layer is sufficiently thick relative to the gap distance to the acceptor. The laser energy is absorbed by the paste layer, creating an vapor bubble that expands in the z-direction towards the acceptor substrate [15]. Before the bubble can burst, it makes contact with the acceptor substrate, thereby avoiding splashing and leaves a small amount of material on the acceptor behind. The size of the transferred material dot can be adjusted with the laser parameters. In the literature the smallest droplet size was reported as 10 μm in diameter [16, 19] which emphasizes the potential of this technology.

The simplified transfer mechanism and donor-acceptor configuration used here is illustrated in Figure 1c. The donor and acceptor slides were separated by a defined spacer made of precisely rolled steel with a thickness of 70 μm. The thickness could be adjusted according to the thickness of the transfer material layer which in our case was 40 μm. The donor slide was a laser-transparent microscope glass that was coated with the paste material to be transferred by doctor blading. The acceptor slide is typically another microscope glass, but it could be exchanged for other substrates, such as silicone or flexible polyimide film.

2.2 | Inks Used for LIFT

The LIFT setup is especially suited for the transfer of high-viscosity inks or pastes onto various substrates. For the fabrication of capacitors, conductive and insulating materials are required. Different inks were tested and bought off the shelf. Silver ink was selected for the printing of capacitors and conductive tracks due to its low resulting electrical resistance. Titanium di-oxide paste was found to be interesting due to the high permittivity, which is reported to be at $\epsilon = 18.9$ as anatase [20], but might deviate due to a different spatial structure.

For the printing of conducting lines and the fabrication of micro-sized capacitors, a silver paste, CL60 by XTPL (Wrocław, Poland), was used. These inks are composed of spherical nanoparticles with a size range of 35–50 nm. Ink CL60 has a silver content of 54 − 63 *wt*. % [21]. The high silver content of this ink promises a good conductivity, which is especially useful for the printing of metal connections. The main solvent used in these inks is a glycol. The viscosity of CL60 is in the range of 30 −50 Pa s at 25°C (shear rate = 0.2 s^{-1}), as specified by the manufacturer [21]. The density of CL60 is in the range of 1.85 −2.50 g cm^{-3}.

For the transfer of the dielectric material, titanium di-oxide paste 791547 supplied by Sigma-Aldrich, Saint Louis, USA, was used. This paste contains titanium dioxide with a content of 17.8%–20.2%. After the transfer, the paste was sintered at 260°C for 180 min to remove the organic solvents. The viscosity of the titanium di-oxide paste is almost similar compared to the silver CL60, ranging from 40 to 55 Pa s [22].

2.3 | Donor Preparation

To prepare donors for LIFT printing with semi-liquid material inks, various strategies can be employed to achieve a thin, homogeneous layer of ink on the slide. In this study, doctor blading was utilized for preparation. Two types of inks were used, with viscosities ranging from 30 to 50 Pa s. The inks were applied to the side of the microscope glass and then spread across the slide using a cylindrical 80 mm wide, TQC Baker film applicator. The applicator was precisely manufactured with gaps of 1010, 1020, 1030, and 1040 μm, fitting for 1000-mm thick microscope glasses, and leading to theoretical film thicknesses of 10, 20, 30, and 40 μm. However, the actual thickness of the coating could vary due to process limitations. A sketch to clarify concepts is shown in Figure 2a. The sweeping movement of the cylinder was carried out using an automated film applicator (TQC Sheen), at a speed setting of 10 mm s^{-1}.

2.4 | Screening for Transfer Parameters

Each ink that was selected for LIFT printing had different properties, which made it necessary to first screen for a set of transfer parameters that would be sufficient for the printing of devices. For the screening, a matrix made up of dots with equal separation was printed, with parameters covering a variation of laser power and laser duration. Each printed dot thus possessed its own set of transfer parameters. These variations lead to different dot sizes for the printed material. The study was done for XTPL CL60 silver ink. A printing window, which consisted of a range of successful parameters, was received from checking the printing result using a light microscope (see Figure 2c). Within the printing window, a particular dot size was chosen to be used for the printing of capacitors and conductive tracks. The set of parameters, 120 mW and 4 ms, was chosen because of the roundness, size (130-μm spot diameter) and the absence of sprinkles surrounding the spot. Although smaller dots may facilitate higher printing resolution, this can be disadvantageous for the printing of larger surfaces. If the pitch between two neighboring dots is insufficient, the dots will not be printed independently of each other. This may result in the accumulation of heat, which could alter the properties of the ink. This, in turn, could lead to defects in the structure and a reduction in printing quality. Consequently, a larger spot with a larger pitch was selected for the printing of capacitors. The screening for transfer parameters for titanium di-oxide paste followed a similar procedure.

2.5 | Capacitor Printing

The described techniques were used to print capacitors. In prior steps, successful printing parameters were found for XTPL silver ink CL60 and Sigma Aldrich titanium di-oxide paste 791547. For a plate capacitor, two electrodes and a separating dielectric layer are necessary. In this study, the capacitor was printed on predefined areas on the glass slide to enable reliable contact

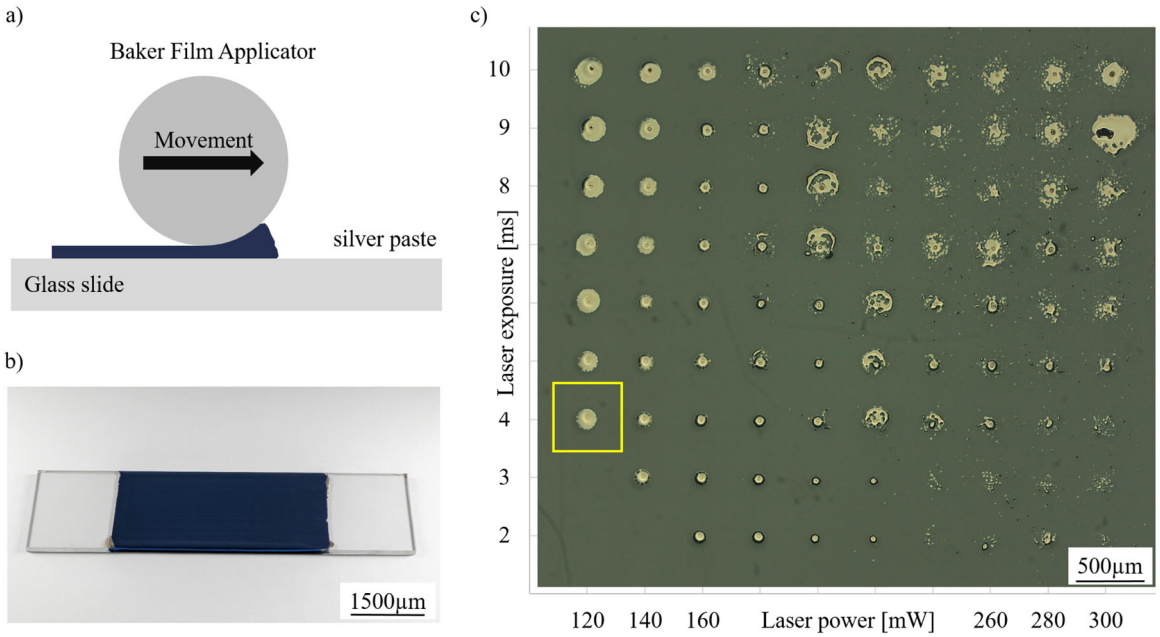

FIGURE 2 | (a) Ink is spread on a face of the microscope glass. The cylindrical Baker film applicator is dragged and distributes the paste over a donor slide. (b) Image of a donor with XTPL CL60 silver ink prepared for the printing process. (c) Screening for transfer parameters: A matrix of material is transferred, with each printed dot having an individual combination of transfer parameters. In the negative *y*-direction, the laser exposure is increased in steps of 1 ms, and in the *x*-direction, the laser power is increased in steps of 20 mW. In this case, 120 mW and 4 ms was selected as optimal (here marked by a yellow box).

with a probestation. The probestation uses a fragile tip with a defined width of 450 µm, and therefore requires the same dimension for the readout structure. These square-shaped areas made of gold were fabricated in a cleanroom process and also serve as bottom electrode of the capacitor. The fabrication of the gold base plates is a lithographic process that involves spin coating of photoresist, mask illumination, and developing. In the next step, a metal stack of 10 nm chromium as an adhesion promoter and 400-nm gold were deposited on the slide. The remaining resist material is removed in an acetone bath. The layout is repetitive, so 8 × 8 capacitors could be printed at once. The layout can be seen in Figure 3a.

The printing of the capacitor was done in two printing steps. First, a layer of titanium di-oxide paste was created. To achieve a larger, connected structure the titanium di-oxide paste was printed dot-by-dot with a laser energy of 200 mW and 2 ms of exposure time. These values were found empirically by printing the screening scheme and choosing a transfer parameter based on the roundness and size of the dots. The pitch is 100 µm that the dots are overlapping and fully cover the gold pad. The dielectric layer was printed slightly larger than the gold pads, as can be seen in Figure 3b, to avoid short circuits.

Before and after the transfer, the paste was still semi-liquid, which is advantageous in this case because the material dots flow into each other, reducing surface roughness. To print the next layer, mixing of two different inks was avoided by performing a sintering step in between. The structures are treated in a vacuum oven at 260°C for 180 min to dry the ink by removing any organic solvent. The vacuum oven helps to maintain standard drying conditions and becomes particularly relevant when treating silver.

In the next printing step, the top electrode out of silver is printed. Again, to create a connected structure, silver dots of XTPL CL60 are printed dot-by-dot with a laser energy of 120 mW and an exposure time of 4 ms. The pitch is 100 µm and chosen to generate an overlap to achieve a connected structure.

To connect the upper electrode to the readout structure, a small conductive track is printed as can be seen in Figure 3c. The printed layer was sintered again at 260°C for 180 min to remove the organic solvents using a vacuum oven. The vacuum also helps to avoid the oxidation and improves the conductivity of the silver.

3 | Characterization

The functionality of the printed capacitors was analyzed by different tools. Conductivity values before and after sintering were determined by impedance measurements, and the layer integrity was checked by focused-ion-beam (FIB) in combination with Scanning Electron Microscope (SEM). An electrical analysis was done to check the frequency dependent capacitor properties.

3.1 | SEM Analysis

The printed capacitors were investigated using an FEI Helios Dual Beam SEM, which can simultaneously perform two tasks of milling trenches, and generating high-resolution images. The device uses Gallium ions for milling, and a scanning electron beam for imaging. To obtain cross-sectional views, the FIB-SEM was used to mill a trench in the capacitor. To protect the sample

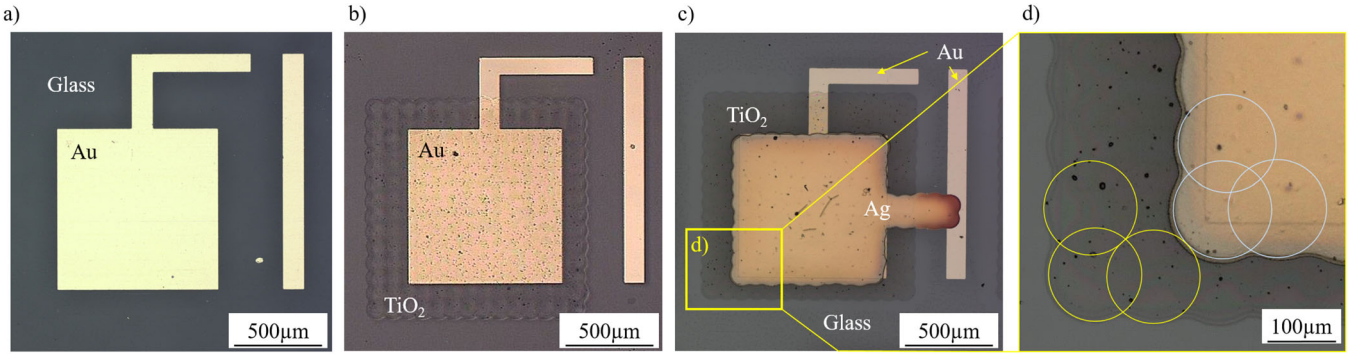

FIGURE 3 | (a) Gold pads are used as base electrodes for printing capacitors. The electrode is designed to fit the contacting tip of the probestation. The gold square is 1 mm^2 and the width of the tracks is 130 μm. The gap between the electrodes is 200 μm. (b) The first printed layer is titanium di-oxide paste. It was printed with an overlap to prevent shorting of the electrodes on the sides. (c) The second printed layer out of silver paste completes the plate capacitor. A conductive track was printed to connect it to the readout electrode. (d) Zoomed-in image of the capacitor to enhance the view of the single printed dots. Titanium di-oxide dot location is indicated by yellow and silver by white circles. Dots are flowing into each other and smoothing the surface.

from ions and to achieve a more precise cut, an additional layer of palladium was deposited from a precursor gas. After milling the trench, the sample was tilted by approximately 52°, before the SEM image was taken. In Figure 4c, it can be seen that the different printed ink materials generated good material contrast, making the layers easy to distinguish. The layer thicknesses can be derived from the image, measuring 1.49 µm for the titanium di-oxide, and 1.36 µm for the silver, with tilt correction of 52° applied. The thickness of the bottom electrode can't be derived from this image, but is known to be 40 nm from the deposition process by evaporation. The interfaces of the layers appeared seamless, with no delamination observed. The inner structure of the layers showed porosity, which is expected because organic solvents and volatile components form cavities in the ink during drying and heat treatment, and the spherical metal particles did not completely melt. The porosity is a limiting factor for capacitor performance, as porous structures typically have higher electrical resistance, and porous dielectric materials have a lower dielectric constant.

3.2 | Resistance Measurements

The resistivity measurements were conducted to determine the electrical performance of printed silver ink used to fabricate capacitor plates. To minimize contact resistance and ensure accuracy, a four-point probe connected to a Keithley 2450 Source Measure Unit (SMU) was used, as depicted in Figure 4b. The silver ink was printed as conductive tracks between two lithographically-formed gold bond pads with lengths of 500 and 1000 µm. After optimizing the pitch value for uniformity, the printing was done at 220-mW laser power, 4-ms exposure, and a pitch of 90 µm. Moreover, the impact of printing two layers on top of each other on conductivity was assessed. Sixteen conductive tracks, one of which is shown in Figure 4a, with identical transfer parameters, were printed for each experimental variation. Electrical resistance was measured before and after sintering. The sintering process involved two steps: raising the temperature by 4°C min^{-1} until reaching a plateau at 100°C, and maintaining it for 5 min, then raising the temperature by 2. 5°C min^{-1} until reaching 250°C, and maintaining it for 30 min, followed by gradual cooling back to room temperature. The resistance was measured by applying a DC through the outer probes, while measuring the voltage drop across the inner probes. Using the measured geometrical parameters, the resistivity of the material was calculated. Table 1 presents the mean resistivity and standard deviation for 16 identical structures measured. As demonstrated in Table 1, sintering significantly improved the conductivity of both single- and double-printed layers, with an average resistivity of 1×10^{-7} Ωm and high repeatability. Single-printed layers showed higher resistivity than double-printed layers. Shorter Ag lines demonstrated lower resistivity compared to longer tracks before and after sintering. These results highlight the significance of double printing in achieving low resistivity for metal tacks, especially in device fabrication. Additionally, sintering greatly reduced the variability in resistivity across the identical structures. Overall, the printing quality was assessed as good, because no physical gaps were observed that would result in an open circuit during electrical measurements. The performance of the printed structures was evaluated by comparing their resistance with that of bulk silver 1.47×10^{-8} Ωm [23], and printed silver from the XTPL datasheet 5.1×10^{-8} Ωm [21]. With an average measured resistance of 1.25×10^{-7} Ωm the value remained close to the manufacturer's data, and 8.5× higher than bulk silver. This was an expected value, taking into account the porosity of the silver as depicted in Figure 4c, which increases resistivity. The good conductive behavior makes this ink especially useful for the printing of conductive tracks or capacitors.

3.3 | Capacitor Performance

The capacitors were evaluated using a network analyzer (Agilent E5061B) and a probe station (Cascade Microtech MPS150) set up with a Z-probe (Z0-20-K3N-GS-500, Cascade Microtech GmbH) to investigate the frequency behavior of capacitor parameters. A calibration was carried out before the measurements with the Z-probe doing open circuit, closed circuit, and 50 Ω measurements using an impedance standard substrate. After the setup, the array of capacitors was measured by contacting the gold tracks fabricated for that purpose. The

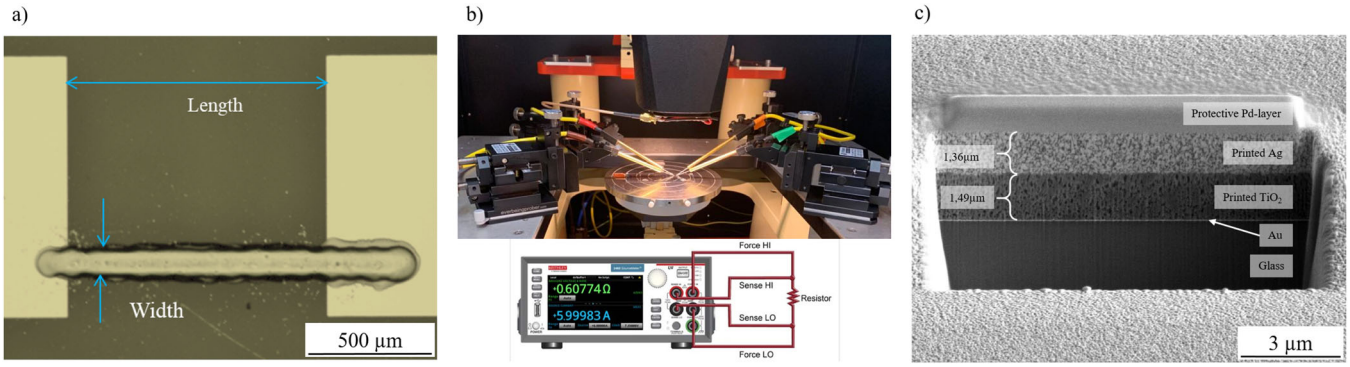

FIGURE 4 | (a) Conductive lines of XTPL silver CL60 printed in an array format with 16 identical lines each between gold conductive pads with lengths of either 500 or 1000 µm. The lines were printed dot-by-dot with a laser power of 220 mW and a 4-ms exposure time. The pitch was 90 µm. These lines were used to measure resistance before and after sintering. (b) The resistance was measured with a four-point probe station connected to a Keithley 2450 Source Measure Unit. (c) The layer integrity of the capacitor is characterized with a focused-ion-beam (FIB) scanning-electron-microscope (SEM).

TABLE 1 | Geometrical properties and measured electrical resistivity of printed conductive lines before sintering (B.S.) and after sintering (A.S.).

Length [µm]	Layers	Height [µm]	Width [µm]	ρ_{mean} [Ωm] B.S.	Std	ρ_{mean} [Ωm] A.S.	Std
1000	1×	2.8	130	1.10×10^{-2}	1.39×10^{-2}	2.15×10^{-7}	7.47×10^{-8}
1000	2×	4.2	130	4.99×10^{-6}	5.38×10^{-7}	1.05×10^{-7}	5.73×10^{-9}
500	1×	1.2	130	3.31×10^{-4}	2.71×10^{-4}	1.33×10^{-7}	3.52×10^{-8}
500	2×	1.6	130	2.31×10^{-5}	3.53×10^{-5}	1.25×10^{-7}	1.78×10^{-8}

capacitors were measured over the frequency range of 1–1000 MHz. Unfortunately, not all capacitors were flawless. The 26% showed visual defects from the printing in the form of missing dots, but still acted as capacitors. Capacitors were counted as such if there was an, s-parameter curve in the lower hemisphere of the Smith chart. A remaining 30% of the devices fulfilled that criterium and didn't show any visual defects. 44% of the capacitors weren't detected as capacitors, but rather were inductive, which can be interpreted as an electrical short between the electrodes. The mean capacity of the 26% of capacitors with visual defects such as missing dots was 36.0 ± 10.3 pF at a frequency of 100 MHz. This is a plausible result because missing dots lead to a smaller electrode coverage and therefore a smaller capacity as well as an increased variance compared to defect free components. The mean capacity over the 30% of working capacitors, that were without visual defects, was 40.1 ± 2.2 pF at a frequency of 100 MHz.

4 | Conclusion and Outlook

The LIFT process demonstrated in this paper represents a versatile and rapid prototyping method for the design and fabrication of capacitors with a wide range of applications. The flexibility of LIFT allows for precise customization of capacitor parameters, such as electrode area and material properties, enabling capacitors to be tailored to specific needs. This makes LIFT-printed capacitors interesting for various electronic applications, particularly where precise capacitance values are required and bulky commercial capacitors cannot be used. A possible application could be as a microdetector for MRI, as described by Nassar, Mager, and Korvink [24], where capacitors for tuning and matching as well as the printing of conductive tracks can be replaced by LIFT. The complexity of the process, that is, inkjet printing combined with electroplating, required to achieve good conductivity, can be reduced to a single printing step.

This paper demonstrated that the LIFT process can fabricate capacitors ranging from 4 pF to few hundred picofarads, with precise control over the design and performance characteristics. For example, the achieved 40 pF with 100 dots could be varied in steps of 1 dot, as shown in Figure 5a–c. The calculated precision of the printed capacitors was approximately 5.5%, highlighting the accuracy and reliability of this method. Parameters such as laser pulse energy, focus conditions or droplet behavior must be analyzed and optimized for a given substrate for higher success rates. Also the long-term stability and repeatability of the process could to be subject of further research. The resolution of 50 µm dots and the dot-by-dot method used in this paper provide more flexibility in transfer, unlike the predecessors [18, 25, 26] who transferred a double layer (dielectric and electrode in one structure) in a square shape.

Looking ahead, the LIFT process opens up significant opportunities for advancing capacitor technology across a variety of industries. The capacity to create capacitors with customizable designs will be especially impactful for high-frequency circuits, advanced medical electronics, and signal processing systems.

Future research should focus on improving the resolution, reliability, and scalability of the LIFT process, potentially by

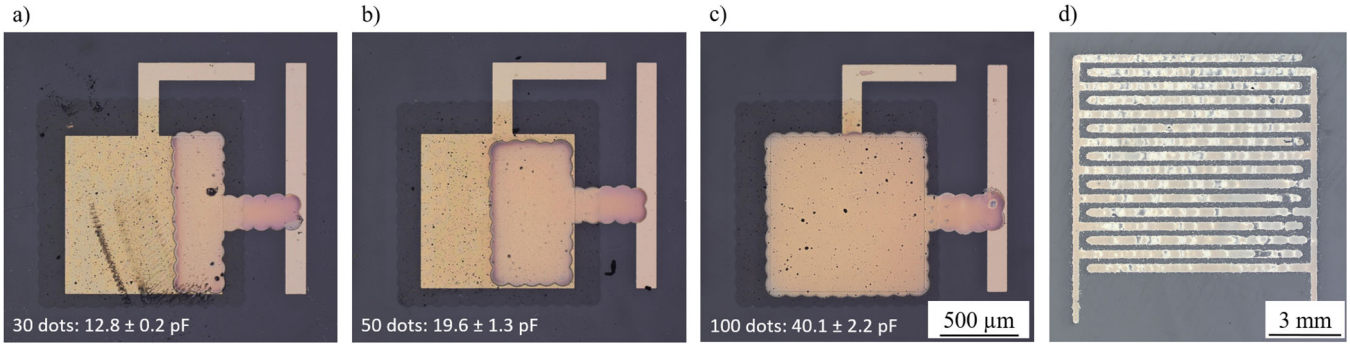

FIGURE 5 | (a)–(c) Capacitors showcasing high design flexibility, where the capacitance value can be adjusted by varying the top electrode's coverage, allowing for precise tuning of the circuit. (d) Demonstration of other capacitor configurations, such as interdigitated layouts, highlighting the versatility of the LIFT process in creating various capacitor designs to meet specific requirements.

enhancing laser technology and exploring new materials. These advancements will extend the possibilities of printed capacitors, particularly the field of miniaturized, printed electronics. Moreover, integrating LIFT-based capacitors into printed electronics on a scale could pave the way for new innovations in personalized electronics, power management, and RF circuits.

In summary, LIFT-based capacitor fabrication holds great promise for revolutionizing capacitor design in modern electronics. For these applications, LIFT offers a precise, adaptable, and rapid solution for creating capacitors that meet the increasingly complex demands of advanced electronics. It also enables the easy design of different types of capacitors, such as interdigitated capacitors (Figure 5d), or other shapes depending on specific requirements. This method is sure to become a key tool for researchers and engineers, offering a new approach to rapid prototyping and precise tuning in electronic circuits.

Acknowledgments

The authors acknowledge the support from the EU under the NANOSTACKS project EXCELLENT SCIENCE—Future and Emerging Technologies (FET) (ID: 951949) for financial support. The authors acknowledge support from the Deutsche Forschungsgemeinschaft (DFG) under Germany's Excellence Strategy—3DMM2O (EXC-2082/1-390761711). We further acknowledge support from the Helmholtz Society's program Materials Systems Engineering, in the Research Area Information. All authors contributed to the revision of the manuscript. Thanks are due to Chaoyu Wu for providing the image of the interdigitated capacitor, and to Markus Breig for the images of the setup.

Conflicts of Interest

Prof. Dr. Frank Breitling is a shareholder of PEPperPRINT GmbH, Heidelberg, a company that markets the LIFT system. The remaining authors declare no conflicts of interest.

Data Availability Statement

The data that support the findings of this study are openly available in KITopen at https://publikationen.bibliothek.kit.edu/, reference number 1000174628.

References

1. J. Ho, T. R. Jow, and S. Boggs, "Historical Introduction to Capacitor Technology," *IEEE Electrical Insulation Magazine* 26, no. 1 (2010): 20–25, https://doi.org/10.1109/MEI.2010.5383924.

2. J. Sun, B. Luo, and H. Li, "A Review on the Conventional Capacitors, Supercapacitors, and Emerging Hybrid Ion Capacitors: Past, Present, and Future," *Advanced Energy and Sustainability Research* 3, no. 6 (2022): 2100191, https://doi.org/10.1002/aesr.202100191.

3. G. L. Brennecka, J. F. Ihlefeld, J.-P. Maria, B. A. Tuttle, and P. G. Clem, "Processing Technologies for High-Permittivity Thin Films in Capacitor Applications," *Journal of the American Ceramic Society* 93, no. 12 (2010): 3935–3954, https://doi.org/10.1111/jace.2010.93.issue-12.

4. S.-w. Chang, J. Oh, S. T. Boles, and C. V. Thompson, "Fabrication of Silicon Nanopillar-Based Nanocapacitor Arrays," Applied Physics Letters 96, no. 15 (2010): 153108, https://doi.org/10.1063/1.3374889.

5. Y. Wang, L. Sun, D. Xiao, et al., "Silicon-Based 3D All-Solid-State Micro-Supercapacitor With Superior Performance," ACS Applied Materials & Interfaces 12, no. 39 (2020): 43864–43875, https://doi.org/10.1021/acsami.0c14441.

6. D. Stüwe, D. Mager, D. Biro, and J. G. Korvink, "Inkjet Technology for Crystalline Silicon Photovoltaics," *Advanced Materials* 27, no. 4 (2015): 599–626, https://doi.org/10.1002/adma.201403631.

7. C. Ru, J. Luo, S. Xie, and Y. Sun, "A Review of Non-Contact Micro- and Nano-Printing Technologies," *Journal of Micromechanics and Microengineering* 24, no. 5 (2014): 053001, https://doi.org/10.1088/0960-1317/24/5/053001.

8. A. Khan, J. S. Roo, T. Kraus, and J. Steimle, *Soft Inkjet Circuits: Rapid Multi Material Fabrication of Soft Circuits Using a Commodity Inkjet Printer* (2019), https://doi.org/10.1145/3332165.3347892.

9. G. Cummins, "Inkjet Printing of Conductive Materials: A Review," *Circuit World* 38 (2012): 193–213, https://doi.org/10.1108/03056121211280413.

10. B. Derby, "Inkjet Printing of Functional and Structural Materials: Fluid Property Requirements, Feature Stability, and Resolution," Annual Review of Materials Research 40, no. 1 (2010): 395–414, https://doi.org/10.1146/matsci.2010.40.issue-1.

11. M. L. Levene, R. D. Scott, and B. W. Siryj, "Material Transfer Recording," *Applied Optics* 9, no. 10 (1970): 2260, https://doi.org/10.1364/AO.9.002260.

12. P. Serra, M. Duocastella, J. Fernández-Pradas, and J. Morenza, "Liquids Microprinting Through Laser-Induced Forward Transfer," *Applied Surface Science* 255, no. 10 (2009): 5342–5345, https://doi.org/10.1016/j.apsusc.2008.07.200.

13. M. Duocastella, J. Fernández-Pradas, J. Morenza, and P. Serra, "Droplet Printing Through Bubble Contact in the Laser Forward Transfer of Liquids," *Applied Surface Science* 257, no. 7 (2011): 2825–2829, https://doi.org/10.1016/j.apsusc.2010.10.070.

14. D. Munoz-Martin, C. Brasz, Y. Chen, M. Morales, C. Arnold, and C. Molpeceres, "Laser-Induced Forward Transfer of High-Viscosity

Silver Pastes," *Applied Surface Science* 366 (2016): 389–396, https://doi.org/10.1016/j.apsusc.2016.01.029.

15. P. Sopeña, J. Fernández-Pradas, and P. Serra, "Laser-Induced Forward Transfer of Low Viscosity Inks," *Applied Surface Science* 418 (2017): 530–535, https://doi.org/10.1016/j.apsusc.2016.11.179.

16. P. Serra and A. Piqué, "Laser-Induced Forward Transfer: Fundamentals and Applications," *Advanced Materials Technologies* 4, no. 1 (2018): 1800099, https://doi.org/10.1002/admt.201800099.

17. J. S. Stewart, T. Lippert, M. Nagel, F. Nüesch, and A. Wokaun, "Red-Green-Blue Polymer Light-Emitting Diode Pixels Printed By Optimized Laser-Induced Forward Transfer," *Applied Physics Letters* 100, no. 20 (2012): 203303, https://doi.org/10.1063/1.4717463.

18. C. Constantinescu, L. Rapp, A. Diallo, C. Videlot-Ackermann, P. Delaporte, and P. Alloncle, "Microcapacitors With Controlled Electrical Capacity in the pF-nF Range Printed by Laser-Induced Forward Transfer (LIFT)," Organic Electronics 20 (2015): 1–7, https://doi.org/10.1016/j.orgel.2015.01.040.

19. M. Duocastella, M. Colina, J. Fernández-Pradas, and Serra, " Study of the Laser-Induced Forward Transfer of Liquids for Laser Bioprinting," Applied Surface Science 253, no. 19 (2007): 7855–7859, https://doi.org/10.1016/j.apsusc.2007.02.097.

20. A. Wypych, I. Bobowska, M. Tracz, et al., "Dielectric Properties and Characterisation of Titanium Dioxide Obtained by Different Chemistry Methods," Journal of Nanomaterials 2014, no. 1 (2014): J.-F. Hochepied, https://doi.org/10.1155/2014/124814.

21. XTPL. *XTPL Silver Ink cl60 Datasheet* (2024), https://xtpl.com/wp-content/uploads/2024/04/XTPL-High-Performance-Materials-Off-shelf-1.pdfXTPL-High-Performance-Materials-Off-shelf-1.pdf.

22. S. Aldrich, Sigma Aldrich 791547, Titania Paste Transparent (2024), https://www.sigmaaldrich.com/DE/de/product/aldrich/791547.

23. C. Poole, Encyclopedic Dictionary of Condensed Matter Physics, Elsevier Science, 2004, https://books.google.de/books?id=CXwrqM2hU0EC.

24. O. Nassar, D. Mager, and J. G. Korvink, "Wireless Double Micro-Resonator for Orientation Free Tracking of MRcatheter During Interventional MRI," *IEEE Journal of Electromagnetics, RF and Microwaves in Medicine and Biology* 5, no. 1 (2021): 78–83, https://doi.org/10.1109/JERM.2020.3010093.

25. C. Constantinescu, L. Rapp, P. Delaporte, and A.-P. Alloncle, "Investigations on Laser Printing of Microcapacitors Using Poly (Methyl Methacrylate) Dielectric Thin Films for Organic Electronics Applications," Applied Surface Science 374 (2016): 90–95, https://doi.org/10.1016/j.apsusc.2015.10.015.

26. C. Constantinescu, L. Rapp, P. Rotaru, P. Delaporte, and A. P. Alloncle, "Polyvinylphenol (PVP) Microcapacitors Printed by Laser-Induced Forward Transfer (LIFT): Multilayered Pixel Design and Thermal Analysis Investigations," Journal of Physics D: Applied Physics 49, no. 15 (2016): 155301. ISSN: 1361-6463, https://doi.org/10.1088/0022-3727/49/15/155301.